

# Electrochemical deposition of yttrium oxide

Igor Zhitomirsky\* and Anthony Petric

Department of Materials Science and Engineering, McMaster University, 1280 Main Street West, Hamilton, Ontario, Canada L8S 4L7. E-mail: zhitom@mcmaster.ca;  
Fax: +1 905 528-9295

Received 13th January 2000, Accepted 14th February 2000

Published on the Web 30th March 2000

Thin films of yttrium hydroxide were obtained from aqueous  $Y(NO_3)_3$  and  $YCl_3$  salt solutions *via* cathodic electrodeposition. The electrodeposition yield was studied under various experimental conditions. By varying the current density, deposition time and yttrium salt concentration, the amount of the deposited material could be controlled. Electrochemical intercalation of poly(diallyldimethylammonium chloride) into the hydroxide deposits has been demonstrated and the mechanism of intercalation has been discussed. The deposits were studied by X-ray diffraction, thermogravimetric analysis and scanning electron microscopy. Formation of crystalline yttrium oxide films from the hydroxide precursor was observed at 600 °C.

## Introduction

The feasibility of cathodic electrolytic deposition of various ceramic materials has recently been demonstrated, including individual oxides and hydroxides,<sup>1–11</sup> complex oxide compounds<sup>1,9,10,12</sup> and composites.<sup>13–15</sup> This method offers important advantages<sup>6,10</sup> and holds promise for various applications.<sup>1,7,15</sup> Cathodic electrodeposition is achieved *via* hydrolysis of metal ions or complexes<sup>6,8,9</sup> by electrogenerated base to form oxide,<sup>1</sup> hydroxide<sup>11,14</sup> or peroxide<sup>6,7</sup> deposits on cathodic substrates. Hydroxide and peroxide deposits can be converted to corresponding oxides by thermal treatment.

Electrodeposition of yttrium oxide films as well as complex oxide films containing yttrium oxide is of considerable interest for electrochemical and electronic applications.<sup>16–18</sup> Matsuda *et al.* investigated electrodeposition of  $Y_2O_3$  in a dimethylformamide solvent containing a small amount of water.<sup>16</sup> However, for applications, requiring electrodeposition from aqueous solutions, it is important to clarify the effect of additives and processing parameters on deposit yield, deposit crystallinity and film morphology. This research, motivated by the importance of yttrium oxide for various applications, also addresses the possibility of electrodeposition of organoceramic materials based on yttrium hydroxide.

The intercalation of organic polymers into ceramics resulted in the development of novel organoceramic nanocomposites.<sup>19–26</sup> These materials exhibit unique mechanical, thermal, electrical, optical and magnetic properties.<sup>20,24,26</sup> Various methods have been used for preparation of organoceramic materials, including melt intercalation,<sup>25</sup> precipitation from aqueous solutions,<sup>23</sup> intercalation polymerization<sup>26</sup> and alternate adsorption.<sup>24</sup> Significant interest has been generated in poly(diallyldimethylammonium chloride) (PDDA) organoceramics.<sup>19,23,24</sup> PDDA is a charged polycation. Recent studies<sup>5</sup> showed the feasibility of electrochemical intercalation of PDDA into thin films prepared *via* cathodic electrodeposition and formation of organoceramic deposits.

This paper presents experimental data on the deposition of yttrium oxide from aqueous solutions and of organoceramic materials from yttrium hydroxide–PDDA *via* cathodic electrodeposition.

## Experimental procedures

Commercial purity  $Y(NO_3)_3 \cdot 5H_2O$  (Aldrich),  $YCl_3 \cdot 6H_2O$  (Alfa Aesar) and poly(diallyldimethylammonium chloride)

(Aldrich) were used as starting materials. A scheme of the structure of PDDA is shown in Fig. 1.

Electrodeposition experiments were performed from aqueous solutions in galvanostatic mode. Cathodic deposits were obtained on chemically cleaned Ni substrates ( $60 \times 60 \times 0.1$  mm) at current densities ranging from 1 to 10 mA cm<sup>-2</sup>. The electrochemical cell used for the deposition process is described elsewhere.<sup>9</sup> After drying at room temperature, the electrolytic deposits were scraped from the Ni electrodes for X-ray diffraction and thermal analysis. Multilayer deposits were obtained by repeated deposition steps (deposition intervals of 15–30 s, and a current density of 5 mA cm<sup>-2</sup>) in which each deposited layer was dried at 200 °C for 5 min on a hot plate. Deposit weights were obtained by weighing the Ni substrates before and after deposition experiments followed by drying at room temperature for 72 h. The phase content was determined by X-ray diffraction (XRD) with a diffractometer (Nicolet I2) using monochromatized Cu K $\alpha$  radiation at a scanning speed of 0.5° min<sup>-1</sup>. Thermogravimetric analysis (TGA) and differential thermal analysis (DTA) were carried out in air between room temperature and 1200 °C at a heating rate of 5 °C min<sup>-1</sup> using a thermoanalyzer (Netzsch STH-409). The microstructures of the deposited films were studied using a Philips 515 scanning electron microscope (SEM).

## Experimental results

Deposits were successfully obtained from aqueous solutions of  $Y(NO_3)_3$  and  $YCl_3$ . Fig. 2 shows the deposit weight *versus* time dependences obtained at constant current density of 5 mA cm<sup>-2</sup>. The weight increase was essentially linear with no appreciable difference between nitrate and chloride baths. Fig. 3 shows the weight of the coating as a function of  $Y(NO_3)_3$  concentration for various current densities. Deposit weight decreases rapidly as the concentration of  $Y(NO_3)_3$  decreases.

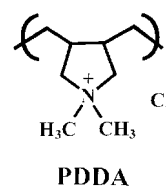
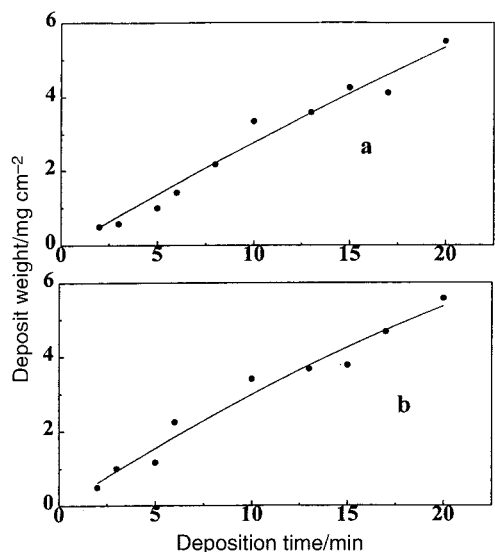


Fig. 1 Schematic structure representation of PDDA.



**Fig. 2** Deposit weight as a function of deposition time at a current density of  $5 \text{ mA cm}^{-2}$  for  $0.02 \text{ M}$  aqueous solutions of  $\text{Y}(\text{NO}_3)_3$  (a) and  $\text{YCl}_3$  (b).

The results given in Fig. 3 indicate that the deposit weight increases with current density at constant deposition time.

The deposits were analyzed by XRD both before and after sintering in air at different temperatures. The fresh deposits and those thermally treated at  $300^\circ\text{C}$  exhibited a very broad peak near  $2\theta \approx 30^\circ$ , but were essentially amorphous (Fig. 4). On sintering the deposits at  $600^\circ\text{C}$  the XRD pattern displayed peaks of  $\text{Y}_2\text{O}_3$  (JCPDS Index Card 25-1200). Thermogravimetric analysis revealed weight loss (Fig. 5) during heating. A sharp reduction of sample weight was observed up to  $\approx 600^\circ\text{C}$ . The total weight loss at  $1000^\circ\text{C}$  was found to be 48.6%. Two endothermic peaks in the DTA curve at around 160 and  $370^\circ\text{C}$  were recorded.

Electrodeposition experiments performed with aqueous PDDA ( $0\text{--}2 \text{ g L}^{-1}$ ) solutions have not revealed deposit formation. However, after the addition of  $\text{YCl}_3$  or  $\text{Y}(\text{NO}_3)_3$  to the PDDA solutions, cathodic deposits were obtained. The data presented in Fig. 6 indicate that deposit weight increased with the increase of  $\text{Y}(\text{NO}_3)_3$  concentration at a constant concentration of PDDA. Higher deposit weights were recorded at higher current density.

Fig. 7 compares the results of TGA of a deposit obtained from mixed  $0.01 \text{ M Y}(\text{NO}_3)_3 + 1 \text{ g L}^{-1}$  PDDA solution with pure PDDA, both dried at room temperature for 10 days. TG curves for the deposit and PDDA show two distinct steps in weight loss. The deposit and PDDA lose weight continuously

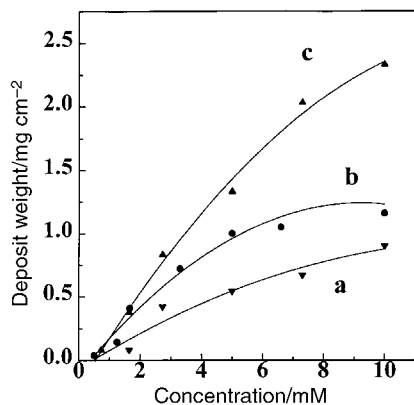


**Fig. 3** Deposit weight as a function of  $\text{Y}(\text{NO}_3)_3$  concentration in aqueous solutions at a constant deposition time of 10 min and a current density of 3 (a), 5 (b) and 10 (c)  $\text{mA cm}^{-2}$ .

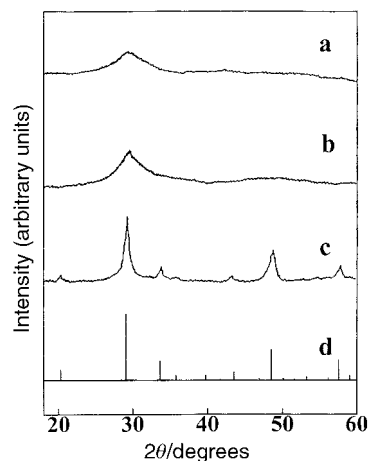


**Fig. 4** X-ray diffraction patterns of the electrolytic deposit obtained from aqueous  $0.01 \text{ M Y}(\text{NO}_3)_3$  solution at a current density of  $5 \text{ mA cm}^{-2}$ : as prepared (a) and after thermal treatment at  $300^\circ\text{C}$  (b),  $600^\circ\text{C}$  (c) for 1 h, compared to JCPDS data file 25-1200 for  $\text{Y}_2\text{O}_3$  (d).

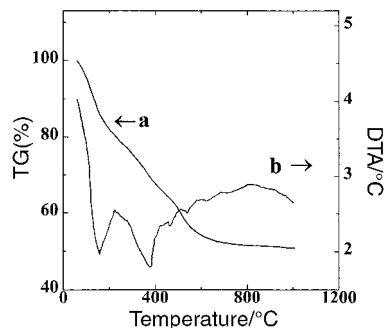


**Fig. 5** TG (a) and DTA (b) data for the deposits obtained at a current density of  $5 \text{ mA cm}^{-2}$  from aqueous  $0.01 \text{ M Y}(\text{NO}_3)_3$  solutions.

until a sharp reduction of weight is observed at  $300^\circ\text{C}$ . The total weight loss for the deposit at  $1000^\circ\text{C}$  was 54.1%. The weight loss for the deposit can be attributed to decomposition of inorganic and organic phases to form yttrium oxide. When considering the deposited material as a mixture of yttrium hydroxide and PDDA, the amount of an organic phase can be evaluated as  $\approx 10.7 \text{ wt.}\%$ .

Thickness of the deposits was in the range up to several microns. However the deposits were porous when their thickness was higher than  $3\text{--}5 \mu\text{m}$ . Thin deposits (up to  $\approx 0.2 \mu\text{m}$ ) of yttrium hydroxide were smooth and crack free. However, cracking was observed when the deposit thickness exceeded  $\approx 0.2 \mu\text{m}$  (Fig. 8). In this work, multi-stage deposition was performed in order to avoid cracking. Yttrium

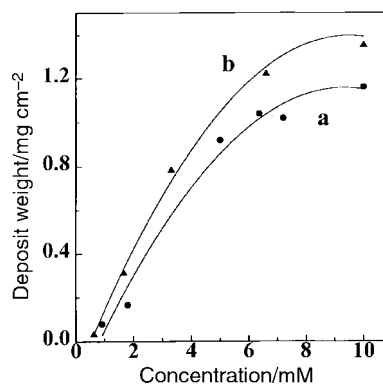


**Fig. 6** Deposit weight as a function of  $\text{Y}(\text{NO}_3)_3$  concentration in aqueous solutions containing  $1 \text{ g L}^{-1}$  PDDA at a constant deposition time of 10 min and a current density of 3 (a) and 5 (b)  $\text{mA cm}^{-2}$ .

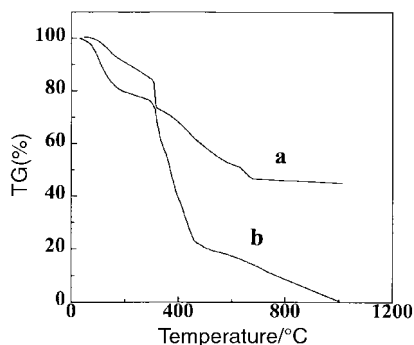


Fig. 7 TG data for deposits obtained from 0.01 M  $Y(NO_3)_3 + 1 \text{ g L}^{-1}$  PDDA solution at current density of  $5 \text{ mA cm}^{-2}$  (a), and for the starting PDDA material (b) dried in air.

hydroxide deposits showed low adhesion to Ni substrates. In contrast, deposits obtained from mixed PDDA containing solutions were adherent to the substrates and exhibited enhanced resistance to cracking. Crack free organoceramic deposits can be obtained as monolayers, when film thickness is in the range up to  $\approx 1 \mu\text{m}$ . Morphologies of the deposits obtained in the presence of PDDA were influenced by the current densities and yttrium salt concentrations. Lower current densities and lower yttrium salt concentrations were preferable in order to obtain more uniform and adherent deposits.

## Discussion

It is known<sup>27,28</sup> that positively charged  $Y^{3+}$ ,  $Y(OH)^{2+}$ ,  $Y_2(OH)_2^{4+}$  species exist in yttrium salt solutions; however  $Y^{3+}$  can be considered as a main yttrium species in acid and neutral solutions.<sup>27</sup> It is supposed that positively charged yttrium species are hydrolyzed by electrogenerated base to form cathodic deposits. According to ref. 27, the yttrium species precipitate as yttrium hydroxide. Therefore, cathodic deposition of yttrium hydroxide could be expected.

The deposit weight was observed to increase with deposition time, as shown in Fig. 2. At this point it should be mentioned that the yield of some other metal hydroxides obtained from chloride baths was found to be greater than the yield obtained from nitrate baths.<sup>2</sup> However, no appreciable difference in deposit weights for nitrate and chloride baths was observed in this work. In dilute solutions, the rate of hydrolysis reactions depends on the rate of diffusion of the reacting species,<sup>1,29,30</sup> detracting from the deposition process efficiency. According to

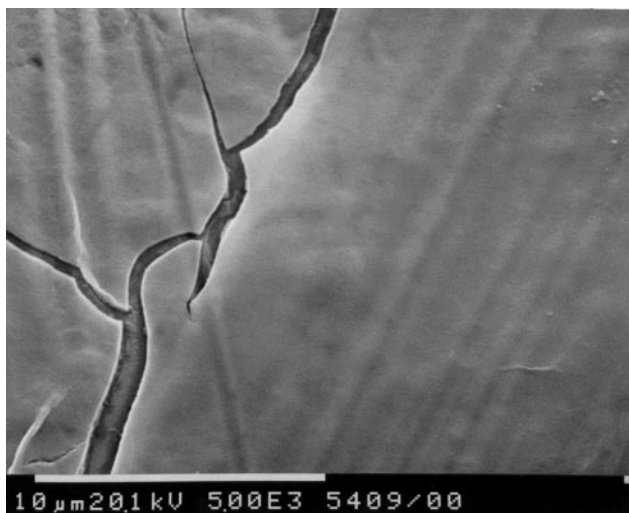


Fig. 8 SEM photo of the electrolytic deposit obtained from 0.01 M  $Y(NO_3)_3$  solution at current density of  $5 \text{ mA cm}^{-2}$ .

ref. 30, the amount of material deposited from dilute solutions is proportional to the square root of deposition time. Therefore, lower deposition rates of yttrium hydroxide can be expected at lower yttrium salt concentrations. Indeed, experiments performed from dilute  $Y(NO_3)_3$  solutions of various concentrations indicate an increase of the deposit weight with the increase of  $Y(NO_3)_3$  concentration (Fig. 3).

Thermal analysis of the deposits revealed weight loss (Fig. 5) which could be attributed to dehydration of the hydroxide deposit to form  $Y_2O_3$ . Observed endotherms could be attributed to different stages in the dehydration of hydroxide precursor. Results of thermal analysis are in a good agreement with the X-ray data, as evidenced by the amorphous nature of fresh deposits and crystallization of  $Y_2O_3$  after thermal treatment at  $600^\circ\text{C}$ .

Cracking was observed in the deposits obtained when the deposit thickness exceeded  $\approx 0.2 \mu\text{m}$ . This cracking is associated with drying shrinkage.<sup>3,9</sup> It is in this regard that deposit microcracking associated with drying shrinkage is a common problem in the wet chemical methods, once thick coatings are formed. In this work, similar to refs. 15 and 31 the cracking problem was approached by multiple deposition. Cracking in ceramic films and green ceramic bodies can be prevented by use of binders. However, the most common binders used in ceramic processing are nonionic type polymers (polyvinyl alcohol, polyvinyl butyral, ethyl cellulose, polyacrylamide, etc.). These polymers are used in electrophoretic deposition<sup>32</sup> where charged ceramic particles provide electrophoretic transport of adsorbed polymeric molecules to form deposits. However, the application of these polymers for electrolytic deposition presents difficulties, as formation of ceramic particles is achieved near the electrode surface.<sup>32</sup> PDDA is a charged polycation (Fig. 1) with inherent binding properties. Therefore, electrophoretic motion of PDDA toward the cathodic substrate can be expected. In a previous investigation<sup>5</sup> the feasibility of electrochemical intercalation of PDDA into a gadolinium hydroxide deposit was demonstrated. It was established that by use of PDDA the problems related to deposit cracking could be diminished. Moreover, the organoceramic material was obtained *via* cathodic electrodeposition.

Electrodeposition experiments performed with aqueous PDDA ( $0\text{--}2 \text{ g L}^{-1}$ ) solutions have not revealed deposit formation, in agreement with previous results.<sup>5</sup> It is important to note that electrophoresis is related to the motion of charged particles toward the electrode, but it is not responsible for the interfacial phenomena related to deposit formation. In this work, cathodic deposits were obtained after the addition of  $Y(NO_3)_3$  or  $YCl_3$  to the PDDA solutions. Deposit weight increased with the increase of yttrium salt concentration at a constant concentration of PDDA, as shown in Fig. 6. Turning again to the experimental data presented in Fig. 3, it is seen that the amount of the yttrium hydroxide deposited from pure  $Y(NO_3)_3$  also increases with the increase of yttrium salt concentration.

The experimental results obtained indicate that PDDA acts as a binder, providing better adhesion of organoceramic deposits and reducing cracking. The amount of an organic phase in deposits obtained from mixed 0.01 M  $Y(NO_3)_3 + 1 \text{ g L}^{-1}$  PDDA solutions at a current density of  $5 \text{ mA cm}^{-2}$  was evaluated as  $\approx 10.7 \text{ wt.}\%$ . However, the experimental data presented in ref. 22 indicate that the organoceramic material obtained by chemical precipitation cannot be considered as a simple mixture of an inorganic material and polymer. The initial degradation of the polymer was observed in the composite.<sup>22</sup>

In previous work,<sup>5</sup> it was suggested that intercalation of polymer particles into the electrolytic deposit was achieved by their adsorption on the surface of colloidal particles, which are produced near the cathode and form a cathodic deposit. A model has been developed<sup>5</sup> based on electrostatic attraction of

oppositely charged colloidal particles of gadolinium hydroxide and polymer. However, according to ref. 33 the attraction between colloidal particles and polyelectrolytes is due to electrostatic, hydrophobic, and dipole-dipole interactions. It was pointed out<sup>5</sup> that the adsorption of polyelectrolytes is a complicated phenomenon, which is influenced by the pH and ionic strength.<sup>34</sup> The attraction of a polyelectrolyte to an oxide surface can be electrostatic and nonelectrostatic or a combination of both.<sup>34</sup> Moreover, chemical bonding was observed between inorganic phases and intercalated polymers.<sup>21,22</sup> It is also expected that electrodeposition of yttrium hydroxide is influenced by polymer intercalation. Indeed, the adsorption of polyelectrolytes on colloidal particles may result in particle bridging and heterocoagulation.<sup>34-37</sup>

It may be noted that particle interaction can be influenced by the electric field, the proximity of the electrode and by electrode reactions. Indeed, coagulation of charged particles can be enhanced by the electric field<sup>38</sup> or by electrohydrodynamic flows.<sup>39</sup> Sader and Chan<sup>40</sup> examined double-layer interaction between spherical particles in the vicinity of a charged flat surface. It was concluded that the proximity of a charged plate could result in reduction or enhancement of the interaction, which is strongly dependent on the electrical properties of the confining plate and of the particles. Therefore, more detailed work, currently under way, is necessary for a better understanding of the mechanism of deposit formation.

Experimental results of this work coupled with the results of previous investigations on zirconia deposition from aqueous solutions<sup>11</sup> pave the way for electrodeposition of yttria-stabilized zirconia films for applications in fuel cells. As pointed out in ref. 10, electrodeposition allows film formation on the atomic scale and is now an important tool in the formation of nanostructured materials.<sup>8,9</sup> Electrolytic coatings are highly uniform, sinter-reactive and offer important processing advantages.<sup>1,6</sup>

## Conclusions

Electrodeposition of yttrium oxide was achieved *via* hydrolysis by the electrogenerated base of  $Y(NO_3)_3$  and  $YCl_3$  salts dissolved in water and thermal decomposition of hydroxide precursor obtained. Results of X-ray and thermogravimetric analysis show that formation of crystalline yttrium oxide from the hydroxide precursor occurs at 600 °C. Films were obtained as monolayers or multilayers. The amount of the deposited material can be controlled by variation of the deposition time, current density and yttrium salt concentration. The electrodeposition process has been quantified in experiments performed with Ni substrates. The experimental conditions were determined for the electrochemical intercalation of positively charged poly(diallyldimethylammonium chloride) into the hydroxide deposits. It was established that the films, obtained from solutions containing the cationic polymer with inherent binding properties as an additive, adhered well to the substrates and exhibited enhanced resistance to cracking. These results pave the way for formation of yttrium oxide films as well as organoceramic films for various applications.

## References

- 1 I. Zhitomirsky, L. Gal-Or, in *Intermetallic and Ceramic Coatings*, ed. N. B. Dahotre and T. S. Sudarshan, Marcel Dekker, Inc, New York, 1999, p. 83.
- 2 G. H. A. Therese and P. V. Kamath, *J. Appl. Electrochem.*, 1998, **28**, 539.
- 3 S. Peulon and D. Lincot, *J. Electrochem. Soc.*, 1998, **145**, 864.
- 4 J. A. Switzer, *Am. Cer. Soc. Bull.*, 1987, **66**, 1521.
- 5 I. Zhitomirsky and A. Petric, *Mater. Lett.*, 2000, **42**, 273.
- 6 I. Zhitomirsky, L. Gal-Or, A. Kohn and H. W. Henniske, *J. Mater. Sci.*, 1995, **30**, 5307.
- 7 I. Zhitomirsky, *J. Europ. Cer. Soc.*, 1999, **19**, 2581.
- 8 I. Zhitomirsky, *Nano Structured Materials*, 1997, **8**, 521.
- 9 I. Zhitomirsky and L. Gal-Or, *J. Europ. Ceram. Soc.*, 1996, **16**, 819.
- 10 I. Zhitomirsky, *J. Europ. Ceram. Soc.*, 1998, **18**, 849.
- 11 I. Zhitomirsky and L. Gal-Or, *J. Mater. Sci.*, 1998, **33**, 699.
- 12 H. Konno, M. Tokita and R. Furuichi, *J. Electrochem. Soc.*, 1990, **137**, 361.
- 13 R. Chaim, I. Zhitomirsky, L. Gal-Or and H. Bestgen, *J. Mater. Sci.*, 1997, **32**, 389.
- 14 R. Chaim, G. Stark, L. Gal-Or and H. Bestgen, *J. Mater. Sci.*, 1994, **29**, 6241.
- 15 I. Zhitomirsky, *J. Mater. Sci.*, 1999, **34**, 2441.
- 16 Y. Matsuda, K. Imahashi, N. Yoshimoto, M. Morita and M. Haga, *J. Alloys and Compounds*, 1993, **193**, 277.
- 17 S. B. Abolmaali and J. B. Talbot, *J. Electrochem. Soc.*, 1993, **140**, 443.
- 18 M. S. Martín-González, J. García-Jaca, E. Morán and M. Á. Alario-Franco, *J. Mater. Chem.*, 1999, **9**, 137.
- 19 Y. Lvov, K. Ariga, I. Ichinose and T. Kunitake, *Langmuir*, 1996, **12**, 3038.
- 20 P. B. Messersmith, P. Osenar and S. I. Stupp, *J. Mater. Res.*, 1999, **14**, 315.
- 21 C. E. Becze and G. Xu, *J. Mater. Res.*, 1997, **12**, 566.
- 22 P. B. Messersmith and S. I. Stupp, *Chem. Mater.*, 1995, **7**, 454.
- 23 P. B. Messersmith and S. I. Stupp, *J. Mater. Res.*, 1992, **7**, 2599.
- 24 E. R. Kleinfeld and G. S. Ferguson, *Chem. Mater.*, 1995, **7**, 2327.
- 25 R. Krishnamoorti, R. A. Vaia and E. P. Giannelis, *Chem. Mater.*, 1996, **8**, 1728.
- 26 P. B. Messersmith and E. P. Giannelis, *Chem. Mater.*, 1993, **5**, 1064.
- 27 J. Van Muylder, in *Atlas of electrochemical equilibria in aqueous solutions*, ed. M. Pourbaix, National Association of Corrosion Engineers, Houston, TX, 1974, p. 177.
- 28 C. W. Bale, A. D. Pelton and W. T. Thompson, *Faculty for the Analysis of Chemical Thermodynamics (FACT2.1) – User Manual*, Thermfact Ltd., Ecole Polytechnique de Montreal, Royal Military College, Montreal, 1996.
- 29 C. C. Streinz, A. P. Hartman, S. Motupally and J. W. Weidner, *J. Electrochem. Soc.*, 1995, **142**, 1084.
- 30 S. Ban and S. Maruno, *Jpn. J. Appl. Phys.*, 1993, **32**, L1577.
- 31 I. Zhitomirsky, A. Kohn and L. Gal-Or, *Mater. Lett.*, 1995, **25**, 223.
- 32 I. Zhitomirsky, *JOM-e*, 2000, **52**(1), in press.
- 33 T. Okubo and M. Suda, *J. Colloid Interface Sci.*, 1999, **213**, 565.
- 34 N. G. Hoogeveen, M. A. Cohen Stuart and G. J. Fleer, *J. Colloid Interface Sci.*, 1996, **182**, 133.
- 35 N. G. Hoogeveen, M. A. Cohen Stuart and G. J. Fleer, *J. Colloid Interface Sci.*, 1996, **182**, 146.
- 36 L. Sjöström and T. Åkesson, *J. Colloid Interface Sci.*, 1996, **181**, 645.
- 37 T. Garino, *J. Am. Ceram. Soc.*, 1992, **75**, 514.
- 38 I. Zhitomirsky and L. Gal-Or, *J. Mater. Sci. Mater. Med.*, 1997, **8**, 213.
- 39 M. Trau, D. A. Saville and I. A. Aksay, *Langmuir*, 1997, **13**, 6375.
- 40 J. E. Sader and D. Y. C. Chan, *J. Colloid Interface Sci.*, 1999, **218**, 423.